

Investigating the solid state hosting abilities of homo- and hetero-valent [Co₇] metallocalix[6]arenes†Seán T. Meally,^a Cecelia McDonald,^a Patrick Kealy,^a Stephanie M. Taylor,^b Euan K. Brechin^b and Leigh F. Jones^{*a}

Received 21st November 2011, Accepted 14th February 2012

DOI: 10.1039/c2dt12229d

A family of homo-valent [Co(II)₇(OH)₆(L₁)₆](NO₃)₂ (**1**), [(MeOH)₂Co(II)₇(OH)₆(L₁)₆](NO₃)₂ (**2**) (where L₁H = 2-iminomethyl-6-methoxyphenol) and hetero-valent [(NO₃)₂Co(III)Co(II)₆(OH)₆(L₂)₆](NO₃)₃MeCN (**4**) (where L₂H = 2-iminophenyl-6-methoxyphenol) complexes possess metallic skeletons describing planar hexagonal discs. Their organic exteriors form double-bowl shaped topologies, and coupled with their 3-D connectivity, this results in the formation of molecular cavities in the solid state. These confined spaces are shown to behave as host units in the solid state for guests including solvent molecules and charge balancing counter anions. Magnetic susceptibility measurements on **2** and **4** reveal weak ferro- and ferrimagnetism, respectively. The utilisation of other Co(II) salt precursors gives rise to entirely different species including the mononuclear and trinuclear complexes [Co(II)(L₂)₂] (**5**) and [Co(III)₂Na(I)₁(L₃)₆](BF₄) (**6**) (where L₃H = 2-iminomethyl-4-bromo-6-methoxyphenol).

Introduction

The design and synthesis of self-assembled molecular flasks and containers capable of encapsulating smaller guest molecules continues to fascinate the scientific community.¹ This is due to their potential applications in both the solution and solid state. Examples of their use in solution include anion sensing² and sequestration,³ catalytic organic transformations,⁴ enzyme mimetics,⁵ drug delivery⁶ and medical diagnostics.⁷ In the solid state interests lie in their potential as gas storage and separation vessels,⁸ and as containers for magnetic nanoparticles towards imaging.⁹ Indeed both organic and metal-organic molecular flasks/containers are well known in the literature. Their formations are driven by a synergistic combination of non-covalent interactions (π - π stacking, H-bonding, ion pairing *etc.*) in the former, and a subtle blend of covalent (metal-ligand bonding) and non-covalent pairings in the latter. The well reported bowl-like calix[*n*]arene cyclophanes ($n = 3, 4, 5, 8$ *etc.*)¹⁰ and their metallocalix[*n*]arene¹¹ structural relations are examples that highlight these differences. Moreover, both of these classes of materials have been reported in the literature to exhibit many of the applications noted above.

Our own work in this field details the solid state guest engagement of highly paramagnetic polynuclear host units, due to their

rarity¹² and potential applications as multifunctional magnetic materials.¹³ To this end we recently reported a family of heptanuclear [M₇] (M = Ni(II), Zn(II)) *pseudo* metallocalix[6]arene host-guest complexes whose self-assembled double-bowl topologies resulted in molecular cavities able to accommodate various guest solvent molecules.¹⁴

Herein we present an extension of this work by showing that we are now able to produce the cobalt analogues of this family and for the first time encourage solid state molecular cavity ingress of anionic guests using a mixed-valence [Co(III)-Co(II)₆] double-bowl. Crystallographic information on complexes **1–4** and **5–6** are documented in Table 1 and S1† respectively. Bond valence sum (BVS)¹⁵ calculations are provided in Table S2†.

Results and discussion

Firstly we highlight the synthesis and characterisation of the double-bowl complexes [Co(II)₇(OH)₆(L₁)₆](NO₃)₂ (**1**) and [(MeOH)₂Co(II)₇(OH)₆(L₁)₆](NO₃)₂ (**2**) (Fig. 1 and 2), built using the ligand 2-iminomethyl-6-methoxyphenol (L₁H) (Scheme 1 (top)). The molecular cavities remain empty in **1** while they are able to accommodate MeOH guests in **2**. Both complexes comprise a central Co(II) ion (Co1) surrounded by six outer ring Co(II) ions (Co2 and symmetry equivalent, *s.e.*), which are all connected *via* μ_3 -bridging OH⁻ anions (O1 and *s.e.*) to form a planar, body-centred, hexagonal core. This {Co(II)₇} topology is known in the literature, however no solid state host-guest properties have been described previously.¹⁶ The six singly deprotonated L₁⁻ ligands bridge the six outer Co(II) ions *via* the $\eta^1:\eta^2:\eta^1:\mu$ -bonding motif. These ligands sit alternately above and below the {Co(II)₇(OH)₆}⁸⁺ plane to form a *pseudo*

^aSchool of Chemistry, National University of Ireland Galway, University Road, Galway, Ireland. E-mail: leigh.jones@nuigalway.ie; Tel: +353 091-49-3462

^bEaStCHEM School of Chemistry, Joseph Black Building, University of Edinburgh, West Mains Road, Edinburgh, EH9 3JJ, Scotland

†Electronic supplementary information (ESI) available. CCDC 843603–843606, 854829 and 854830. For ESI and crystallographic data in CIF or other electronic format see DOI: 10.1039/c2dt12229d

Table 1 Crystallographic data for complexes 1–4

	1	2·2MeOH	3	4·3MeCN
Formula ^a	C ₅₄ H ₆₆ N ₈ O ₂₄ Co ₇	C ₅₆ H ₆₆ N ₈ O ₂₆ Co ₇	C ₁₄ H ₁₃ NO ₂	C ₉₀ H ₈₇ N ₁₂ O ₂₇ Co ₇
<i>M_w</i>	1623.66	1679.68	227.25	2181.23
Crystal system	Trigonal	Trigonal	Orthorhombic	Monoclinic
Space group	<i>P</i> 3̄ <i>c</i> 1	<i>P</i> 3̄ <i>c</i> 1	<i>P</i> 2 ₁ 2 ₁ 2 ₁	<i>C</i> ₂ / <i>c</i>
<i>a</i> /Å	14.110(2)	14.041(2)	6.0471(6)	29.2767(15)
<i>b</i> /Å	14.110(2)	14.041(2)	9.0763(12)	12.9879(5)
<i>c</i> /Å	22.770(5)	23.036(5)	20.933(3)	24.4043(9)
<i>α</i> /°	90	90	90	90
<i>β</i> /°	90	90	90	92.797(2)
<i>γ</i> /°	120	120	90	90
<i>V</i> /Å ³	3926.0(11)	3933.1(11)	1148.9(3)	9268.5(7)
<i>Z</i>	2	2	4	4
<i>T</i> /K	150(2)	150(2)	150(2)	150(2)
<i>λ</i> ^b /Å	0.7107	0.7107	0.7107	0.7107
<i>D_c</i> /g cm ⁻³	1.373	1.418	1.314	1.563
<i>μ</i> (Mo-Kα)/mm ⁻¹	1.511	1.513	0.088	1.306
Meas./indep. (<i>R</i> _{int}) refl.	2353/1767(0.0295)	2362/2188(0.0184)	2000/1347(0.0486)	8489/5388(0.0684)
Restraints, parameters	0, 143	2, 153	0, 143	2, 617
<i>wR</i> ₂ ^c (all data)	0.2796	0.2221	0.1874	0.1693
<i>R</i> ₁ ^{d,e}	0.0851	0.0695	0.0751	0.0697
Goodness of fit on <i>F</i> ²	1.211	1.194	1.015	1.052

^a Includes guest molecules. ^b Mo-Kα radiation, graphite monochromator. ^c $wR_2 = [\sum w(|F_o|^2 - |F_c|^2)|^2 / \sum w|F_o|^2]^2$. ^d For observed data. ^e $R_1 = \sum ||F_o| - |F_c|| / \sum |F_o|$.

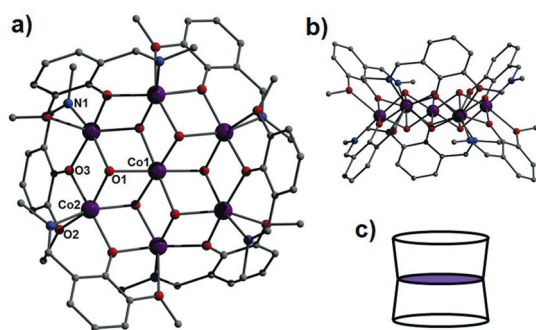


Fig. 1 (a) Crystal structure of **1** as viewed perpendicular (a) and parallel (b) to the planar {Co(II)₇} core. (c) Schematic representation of the double-bowl topology in **1** and its analogues. Colour code (used throughout this work): purple (Co), red (O), blue (N), grey (C). H-atoms and anions omitted for clarity.

metalloalix[6]arene double-bowl (Fig. 1b and c). Crystallographic inspection of these molecular bowls shows dimensions (base × depth × rim diameter) of (Å): 6.27 × 3.96 × 12.89 (**1**) and 6.25 × 4.08 × 12.12 (**2**), respectively.

The molecular cavities formed by the 1D pseudo superimposable columns in the crystal of **2** act as molecular hosts by encapsulating two disordered MeOH guest molecules which are sequestered from the reaction medium. The first methanol guest is disordered over three sites, lying on the 3-fold axis that runs perpendicular to the [Co(II)₇] plane through the central Co(II) centre. The second MeOH guest has 2-fold disorder and lies at the boundary of the molecular cavity in **2**, sitting perpendicular to the [Co(II)₇] plane (Fig. 2). Interestingly the molecular cavities in **1** remain guest free, choosing not to accommodate EtOH solvent molecules – presumably due to steric effects and/or crystallographic restraints (*i.e.* perhaps the kinked nature of the

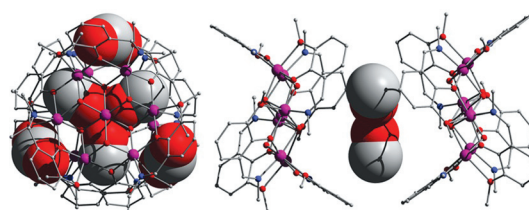
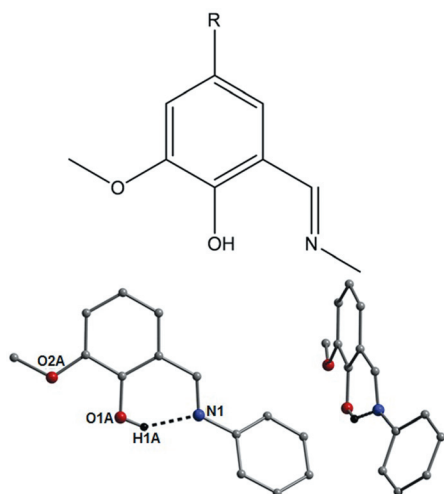


Fig. 2 Space-filled representations of the two crystallographically unique guest MeOH molecules lying within the molecular cavities formed by two double-bowl [Co(II)₇] units in complex **2**.

EtOH molecules cannot satisfy the three-fold symmetry pattern shown by the linear MeOH guests in **2**, as dictated by their identical *P*3̄1/*c* space groups). This is consistent with that observed for the Ni(II) and Zn(II) analogues.¹⁴ Complexes **1** and **2** crystallise in the trigonal *P*3̄*c*1 space group and only differ in terms of their guest occupancy and therefore are analogous with respect to their packing arrangement (Fig. 3). The 1D [Co(II)₇] columns in their unit cells are connected *via* H-bonds to adjacent [Co(II)₇] stacks ([Co(II)₇]_{plane}...[Co(II)₇]_{plane} distances: 11.39 (**1**) and 11.52 Å (**2**)), propagated by multiple interactions between the NO₃⁻ counter anions and the individual [Co(II)₇] moieties (*e.g.* O4...H5(C5) = 2.406 Å in **1**; O4...H7(C7) = 2.431 Å in **2**). More specifically each heptanuclear unit is H-bonded to twelve NO₃⁻ counter anions which in turn connect to six other [Co(II)₇] units thus creating (6,12)-connected nets with (4¹⁵)₂(4⁴⁸.6¹⁸)-**alb** topologies.

In order to further probe the hosting abilities of the heptanuclear hosts and to attract more intriguing guests, we decided to modify L₁H at the imine position *via* introduction of a phenyl group, in order to modulate its second order coordination sphere behaviour upon primary {M(II)₇(OH)₆(L)₆}²⁺ planar disc formation. The ligand 2-iminophenyl-6-methoxyphenol (L₂H (**3**))



Scheme 1 Top: Schematic of the ligands L_1H ($R = H$) and L_3H ($R = Br$) used in this work. Bottom: Crystal structure of the ligand 2-imino-phenyl-6-methoxyphenol (L_2H (**3**)) as viewed perpendicular (left) and along the plane (right) of the phenolic ring. Colour code: grey (C), blue (N), red (O), black (H). Majority of the hydrogen atoms omitted for clarity. Dashed line represents the intramolecular H-bonding interaction in L_2H , measured at $O1A(H1A)\cdots N1 = 1.887 \text{ \AA}$.

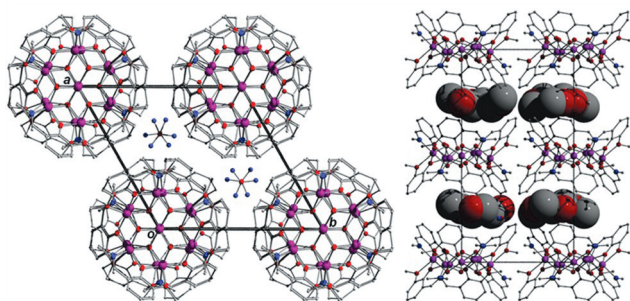


Fig. 3 Left: Packing observed in $[Co(II)_7(OH)_6(L_1)_6](NO_3)_2$ (**1**) as viewed down the c axis of the unit cell, highlighting the 1D columns observed in **1** (and **2**). Right: Crystal packing observed in $[(MeOH)_2CCo(II)_7(OH)_6(L_1)_6](NO_3)_2$ (**2**). The MeOH guests are space-fill represented.

can be easily synthesised (see the Experimental section for details) through the Schiff base condensation of *o*-vanillin and aniline. L_2H crystallises in the orthorhombic $P2_12_12_1$ space group ($Z = 4$) and possesses an intramolecular H-bond between the phenolic proton (H1A) and the imine nitrogen atom (N1), giving a distance of $O1A(H1A)\cdots N1 = 1.887 \text{ \AA}$ and hydrogen bond angle of 144.9° . Furthermore the imino-phenyl and phenol rings of L_2H (as perhaps expected) twist away slightly from one another (*via* the imine bridge) to give a staggered conformation with a torsion angle ($C10-C9-N1-C8$) of 30° . Although structural analogues to L_2H (**3**) have been crystallographically reported with various substituents on the imino-phenyl ring,¹⁷ we present here the first crystal structure of this particular ligand (Scheme 1). Upon reaction with $Co(NO_3)_2 \cdot 6H_2O$ and NaOH in MeOH the first example of a mixed-valence analogue of our $[M(II)_7]$ double-bowl *pseudo* metallocalix[6]arenes, $[(NO_3)_2CCo(III)Co(II)_6(OH)_6(L_2)_6](NO_3) \cdot 3MeCN$ (**4**), is formed.

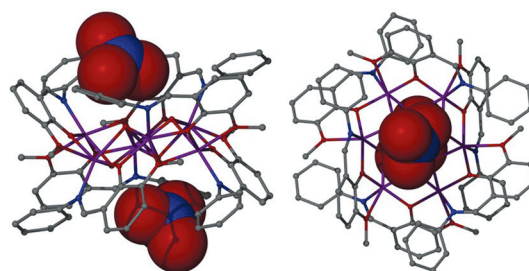


Fig. 4 Crystal structure of the mixed-valent complex $[(NO_3)_2CCo(III)Co(II)_6(OH)_6(L_2)_6](NO_3) \cdot 3MeCN$ (**4**) as viewed parallel (left) and perpendicular (right) to the $\{Co(III)Co(II)_6\}$ plane. Guest NO_3^- anions are space-fill represented.

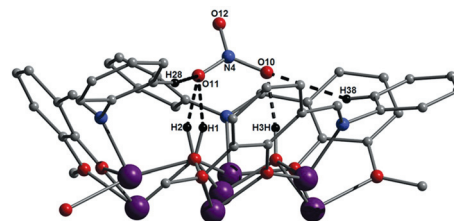


Fig. 5 View of a NO_3^- anion occupying one half of a double-bowl $[Co(III)Co(II)_6]$ unit in **4**. Intermolecular interactions between the host and guest are represented as dashed lines. Actual distances are given in the main text.

Complex **4** (Fig. 4) differs to its $[M(II)_7]$ siblings in that its central Co ion is in the +3 oxidation state, as confirmed by bond length and charge balance considerations and BVS analysis (Table S2†). The metal–oxygen core of the molecule is thus $\{Co(III)Co(II)_6(OH)_6\}^{9+}$. As a result of this extra +1 charge, complex **4** is able to accommodate two of its three counter NO_3^- anions within its double-bowl cavities which is driven by the resultant $\{Co(III)Co(II)_6(OH)_6(L_2)_6\}^{3+}\cdots NO_3^-$ electrostatic interactions. Indeed this observation is a first for such *pseudo* metallocalix[6]arene systems. It should also be noted that complex **4** is the only polymetallic complex to be isolated using ligand L_2H (**3**), having previously produced only monomeric species of Re, Ru and Co.^{18–20} The two symmetry equivalent NO_3^- guests are held in position *via* their O-atoms (O10–12) by four interactions in the form of two long C–H \cdots O contacts from the phenyl ring of the L_2^- ligands ($C28(H28)\cdots O11 = 2.969 \text{ \AA}$; $C38(H38)\cdots O10 = 2.653 \text{ \AA}$) and three H-bonds formed with donor protons (H1, H2 and H3H) of the bridging μ_3-OH^- ions within the $\{Co(III)Co(II)_6\}$ core ($O1(H1)\cdots O11 = 2.280 \text{ \AA}$; $O2(H2)\cdots O11 = 1.916 \text{ \AA}$ and $O3(H3H)\cdots O10 = 1.802 \text{ \AA}$), giving H-bond angles of 123.60 , 146.98 and 170.50° , respectively (Fig. 5). The C–H \cdots O interactions described here are made possible by the staggered conformation of the two aromatic rings (phenolic *versus* imine-phenyl) of each L_2^- ligand upon metallation (torsion angles now ranging from ~ 49 to 76° *cf.* 30° in unbound L_2H); thus giving rise to a more distorted double-bowl shape compared to our $[M(II)_7]$ analogues. Moreover the role of the imine-phenyl groups in **4** should not be underestimated in terms of driving the observed anion inclusion, thus highlighting the importance of ligand choice/design and the resulting cavity size and shape in this work.

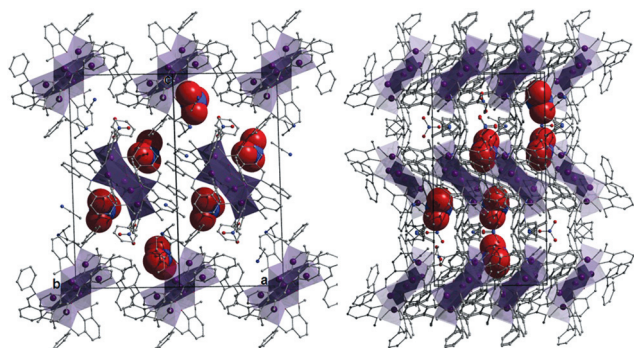


Fig. 6 Crystal packing illustrations of **4** as viewed across the *ab* plane (left) and down the *a* axis (right) of the unit cell. Only guest NO_3^- anions are shown here (in space-fill mode).

In terms of intermolecular connectivity between the individual $[\text{Co}(\text{III})\text{Co}(\text{II})_6]$ units the O-atoms (O12 and s.e.) of the guest NO_3^- anions form close contacts with aromatic (H10) and aliphatic (H29C) ligand protons ($\text{C10}(\text{H10})\cdots\text{O12} = 2.439 \text{ \AA}$, $\text{C29}(\text{H29C})\cdots\text{O12} = 2.627 \text{ \AA}$). The third NO_3^- counter ion lies outside the confines of the double-bowls and acts as another connector of multiple $[\text{Co}(\text{III})\text{Co}(\text{II})_6]$ units *via* C–H \cdots O interactions, through the aromatic ligand protons (H3, H4 and H21) at distances of $\text{C3}(\text{H3})\cdots\text{O14}' = 2.449 \text{ \AA}$, $\text{C4}(\text{H4})\cdots\text{O14} = 2.564 \text{ \AA}$ and $\text{C21}(\text{H21})\cdots\text{O13} = 2.357 \text{ \AA}$. Interestingly the individual double-bowl $[\text{Co}(\text{III})\text{Co}(\text{II})_6]$ units in **4** do not stack upon one another to form the enclosed molecular cavities observed in the related $[\text{M}(\text{II})_7]$ host–guest analogues.¹⁴ Instead these units lie perpendicular to one another within the unit cell and pack in wave-like rows along the *c*-axis. These individual rows arrange in a parallel fashion along the *a* direction of the unit cell with alternating wave phases (Fig. 6). Complex **4** is only the second mixed-valence $\{\text{Co}(\text{III})\text{Co}(\text{II})_6\}$ structure to be reported²¹ and is the first to show such solid state host–guest behaviour. Interestingly the formation of **4** in relation to **1** and **2** represents (to our knowledge) the first example whereby Co(II) oxidation is observed while the exact polynuclear core structure is retained.

The production of **4** prompted our focus to shift towards solid state guest inclusion of other counter anions using our $[\text{Co}(\text{III})\text{Co}(\text{II})(\text{L}_2)_6]^{2+}$ “vessel”. The first candidate was the O-rich SO_4^{2-} anion in the hope of interaction with our H-rich planar core (containing six OH^- bridges). We were also curious to know what would occur when we added a doubly negative anion. However SO_4^{2-} cavity ingress was not observed. Indeed the synthesis of $[\text{Co}(\text{II})(\text{L}_2)_2]$ (**5**) (crystallising in the monoclinic $P2_1/c$ space group upon reaction of $\text{CoSO}_4 \cdot 7\text{H}_2\text{O}$, L_2H and NaOH in MeOH) does not contain our anion and instead comprises a single distorted tetrahedral Co(II) ion (Co1) bound by two crystallographically unique L_2^- ligands. These ligands chelate the Co(II) ion *via* their imine N atoms (N1 and N2) and O_{phen} atoms (O2 and O4) with bite angles of 94.32° (N1–Co1–O2) and 96.51° (N2–Co1–O4). The $\{\text{Co}(\text{II})(\text{L}_2)_2\}$ moieties in **5** are arranged in superimposable rows along the *c* axis of the unit cell. These are held together *via* multiple H-bonds between aromatic protons (H11 and H12 from same L_2^-) and O_{phen} (O2) and OMe (O3) oxygen atoms as shown in Fig. 7 ($\text{O2}\cdots\text{H11}'(\text{C11}') = 2.660 \text{ \AA}$; $\text{O3}\cdots\text{H12}'(\text{C12}') = 2.568 \text{ \AA}$). On closer inspection the H-bonding in **5** is extensive with each monomeric unit

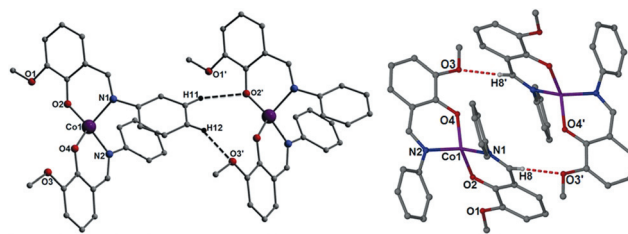


Fig. 7 Crystal structure of $[\text{Co}(\text{II})(\text{L}_2)_2]$ (**5**) highlighting the close proximity of neighbouring monomers within the H-bonded chains (left) and between the chains (right). H-bonding shown using dashed lines.

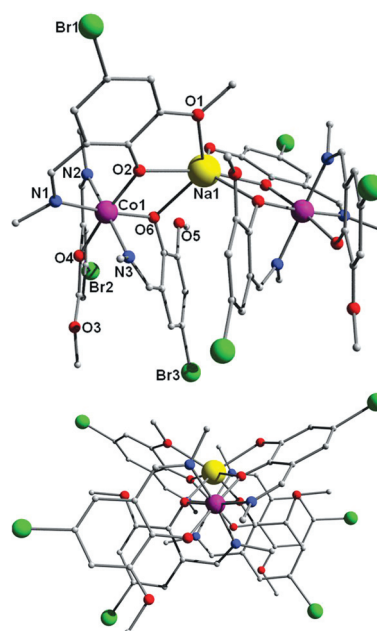


Fig. 8 Crystal structures of $[\text{Co}(\text{III})_2\text{Na}(\text{I})_1(\text{L}_3)_6](\text{BF}_4)$ (**6**) as viewed perpendicular (top) and parallel (bottom) to the V-shaped plane of the molecule. Colour code: purple (Co), yellow (Na), red (O), blue (N), green (Br) and grey (C). H-atoms and anions omitted for clarity.

interacting with four near monomeric neighbours. The superimposable rows propagating along *c* are also involved in inter-chain H-bonding (along the *ab* cell plane), again using aromatic L_2^- protons (H18, H8) and O_{phen} (O2) and OMe (O4) donor atoms ($\text{C18}(\text{H18})\cdots\text{O2}' = 2.571 \text{ \AA}$; $\text{C8}(\text{H8})\cdots\text{O3}' = 2.491 \text{ \AA}$) (Fig. S2†).

Undeterred by the unexpected production of **5**, we decided to attempt to incorporate the tetrahedral BF_4^- counter anion within the $\{\text{Co}(\text{III}/\text{II})_7\}$ complexes of **1**, **2** and **4** by repeating their general synthetic preparations using the $\text{Co}(\text{BF}_4)_2 \cdot 6\text{H}_2\text{O}$ salt precursor. Our thoughts were that by incorporating this particular anion we would perhaps: (1) modify the crystal space group and the size and shape of the resultant molecular cavity and/or (2) encourage the proton-acceptor F-atoms of the BF_4^- anion to occupy the molecular cavities *via* interactions with the OH^- bridging protons located within. However, this approach again failed, and instead the complex $[\text{Co}(\text{III})_2\text{Na}(\text{I})_1(\text{L}_3)_6](\text{BF}_4)$ (**6**) was formed. Complex **6** (Fig. 8) crystallises in the monoclinic $C2/c$ space group in $\sim 25\%$ yield and comprises a V-shaped metal–oxygen core whereby a central Na(I) ion (Na1) sits in

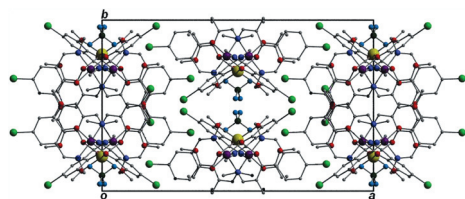


Fig. 9 Crystal packing observed in **6** as viewed along the *c* axis. Hydrogen atoms omitted for clarity. Colour code: yellow (Na), purple (Co), red (O), dark blue (N), grey (C), green (Br), dark green (B), light blue (F).

between two Co(III) centres (Co1 and s.e.). Six L_3^- ligand units bridge the $\{Co(III)_2Na(I)\}$ core in **6**, two of which chelate the Co(III) ions (bite angle: $N2-Co1-O4 = 91.36^\circ$); one per crystallographically unique ion. The remaining four L_3^- ligands bridge the Co(III)–Na(I) vertices, two *via* the $\eta^1:\eta^2:\eta^1:\mu$ -coordination mode and two *via* the $\eta^1:\eta^2:\mu$ -bridging mode (Fig. 8). The BF_4^- anions in the unit cell of **6** sit above the central Na(I) centres ($B1\cdots Na1 = 4.537 \text{ \AA}$) and partake in hydrogen bonds *via* the ligand protons ($H18B$ and $H8$) and the F-atoms ($F1$ and $F2$) with distances of $F1\cdots H18B(C18) = 2.915 \text{ \AA}$ and $F2\cdots H8(C8) = 2.442 \text{ \AA}$. These interactions along with their symmetry equivalents effectively connect the individual $\{Co(III)_2Na(I)\}$ units in **6** which pack in the common brickwall fashion along the *ab* plane of the unit cell. These 2-D sheets then lie parallel to one another along the *c* axis and each is inverted with respect to their neighbouring wall (Fig. 9).

Magnetic susceptibility studies

Magnetic susceptibility studies on **2** and **4** were performed in the 5–300 K temperature range in an applied field of 0.1 T (Fig. 10). Both show similar behaviour at high temperatures with broad maxima (at ~ 100 K) reflecting the effects of spin–orbit coupling. At ~ 40 K however the two curves diverge. For **2** the value of $\chi_M T$ increases with decreasing temperature reaching a value of $\sim 20.2 \text{ cm}^3 \text{ K mol}^{-1}$ at 5 K, suggestive of weak ferromagnetic exchange, while that for **4** decreases with temperature reaching $\sim 13.9 \text{ cm}^3 \text{ K mol}^{-1}$ at 5 K, indicating weak antiferromagnetic exchange. This analysis is corroborated by examining the low temperature field-dependence of the magnetisation (Fig. 10 – inset) which shows that for the same temperature and field, the magnetization value of complex **2** is always larger than that of complex **4**. An examination of the crystal structure of **4** reveals that the Co–O–Co angles in the magnetic $[Co(II)_6]$ wheel fall into two distinct categories: those on the outer rim (OR) are in the range $105.5\text{--}107.4^\circ$ and those on the inner rim (OH) are in the range $95.5\text{--}96.3^\circ$. The former are expected to propagate anti-ferromagnetic interactions and the latter ferromagnetic interactions.^{22,23} On moving from complex **4** to complex **2** the inner rim μ_3 -bridging OH ions now also bridge to the paramagnetic central ion and these Co–O–Co angles are also in the range ($94.0\text{--}98.0^\circ$) expected for ferromagnetic exchange. The conclusion therefore is that the larger outer rim angles dominate the exchange in **4** leading to overall weak antiferromagnetic exchange but the larger number of smaller inner rim angles present in **2** result in global ferromagnetic exchange.

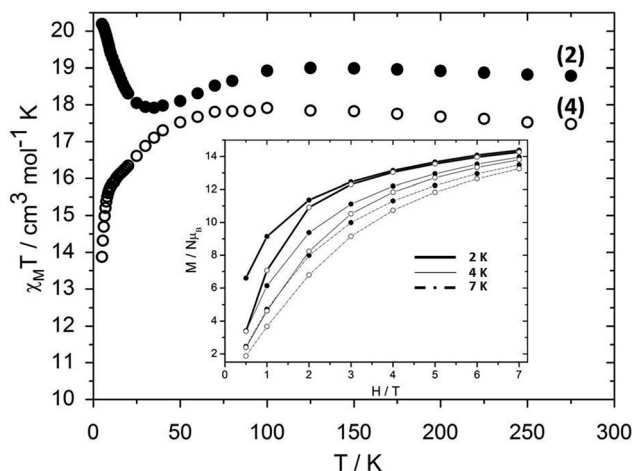


Fig. 10 Plots of $\chi_M T$ vs. T obtained from polycrystalline samples of **2** (●) and **4** (○) measured in an applied field of 0.1 T. Inset: Plot of $M/N\mu_B$ vs. H/T for **2** (●) and **4** (○) at 2, 4 and 7 K, in fields between 0.5–7.0 T. Solid lines are a guide to the eye

Solution studies on **2** and **4**

UV-visible solution studies on **2** and **4** in MeCN and MeOH each show transitions at ~ 260 , ~ 230 and ~ 200 nm and are indicative of $\pi \rightarrow \pi^*$ excitations. Absorptions observed at wavelengths centred on the 350–365 nm region in both MeOH and MeCN solutions of **2** and **4** are attributed to $n \rightarrow \pi^*$ excitations (Fig. S5 and S6†). ESI-MS measurements on a MeOH solution of **2** gave a parent peak at $m/z = 777.8$ which is consistent with the $[Co(II)_7(OH)_2(OMe)_4(L_1)_6]^{2+}$ fragment. Indeed similar bridging ligand substitutions have been observed in previously reported analogues.^{16b} The behaviour of **4** in a MeCN solution gave rise to major fragments at (m/z) 623.7, 966.6 and 1995.1, which are attributed rather neatly to the presence of the $[Co(III)Co(II)_6(OH)_6(L_2)_6]^{3+}$, $[Co(III)Co(II)_6(OH)_6(L_2)_6+(NO_3)]^{2+}$ and $[Co(III)Co(II)_6(OH)_6(L_2)_6+(NO_3)_2]^+$ species, respectively (Fig. S7†). It should be noted here that although the solubility of **1**, **2** and **4** (and all other previously reported $[M(II)_7]$ ($M = Ni, Zn$) siblings) were adequate for UV-vis and MS evaluations, their poor solubility at higher concentrations unfortunately rules out any solution state host–guest measurements (*i.e.* NMR titration studies).

Conclusions

The production of the metallocalix[6]arene $[Co(II)_7]$ discs **1** and **2** highlights the consistent and reproducible nature of our recently reported $[M(II)_7]$ ($M = Co, Ni, Zn$) family of host–guest complexes.¹⁴ Indeed the reproducibility, stability and retainment of this core topology, despite moving across the 1st row of the d-block, is extremely rare with respect to polynuclear assemblies.²³ By varying the ligand employed we are able to encourage the accommodation of guest anionic species and the formation of analogous compounds containing different oxidation state distributions (*e.g.* complex **4**). These changes also have a dramatic effect upon the observed magnetic properties, switching antiferromagnetic exchange in the mixed-valence complex to ferromagnetic exchange in the homo-valent complex. Attempts at

replacing the anion failed, and instead gave rise to the very different complexes **5** and **6**. These latter findings highlight the fine balance that exists between the formation of different complexes and how the identity of the product is dependent upon (1) the starting materials present (the type and the number), (2) the reaction conditions and (3) the crystallisation methods. In this particular case it is apparent that the presence of the NO_3^- anion has significant bearing on $[\text{Co}_7]$ double-bowl *pseudo* metallocalix[6]arene formation.

Experimental section

Variable-temperature, solid state direct current (dc) magnetic susceptibility data down to 1.8 K were collected on a Quantum Design MPMS-XL SQUID magnetometer equipped with a 7 T dc magnet. Diamagnetic corrections were applied to the observed paramagnetic susceptibilities using Pascal's constants. Each sample was encased in an Eicosane matrix to prevent torquing. CHN microanalysis was carried out at the School of Chemistry, NUI Galway. ESI-MS was carried out using a Waters LCT Premier XE system coupled with a Waters E2795 separations module.

All solvents and reagents were used as received without further purification. *Caution*: Although no problems were encountered in this work great care must be taken when working with the potentially explosive nitrate salts.

$[\text{Co}(\text{II})_7(\text{OH})_6(\text{L}_1)_6](\text{NO}_3)_2$ (**1**)

To a conical flask (100 cm^3) containing 30 cm^3 of EtOH was added $\text{Co}(\text{NO}_3)_2 \cdot 6\text{H}_2\text{O}$ (0.25 g 0.86 mmol), NaOH (0.034 g, 0.86 mmol) and 2-iminomethyl-6-methoxyphenol (0.14 g, 0.86 mmol). The resultant dark purple solution was agitated for 2 h and then filtered. Purple hexagonal crystals of **1** were obtained upon slow evaporation of the filtrate after 1 week in 5% yield. Elemental analysis calculated for $\text{C}_{54}\text{H}_{66}\text{N}_8\text{O}_{24}\text{Co}_7$ (%): C 39.95, H 4.10, N 6.90; found: C 40.02, H 3.88, N 6.86. FT-IR (cm^{-1}): 3429(w), 3067(w), 2931(w), 2038(w), 1628(m), 1604(m), 1561(w), 1475(m), 1457(m), 1407(m), 1335(m), 1305(s), 1241(m), 1221(s), 1670(m), 1149(w), 1091(m), 1074(m), 1013(m), 961(m), 883(w), 859(m), 830(w), 787(m), 743(s).

$(\text{MeOH})_2 \subset \text{Co}(\text{II})_7(\text{OH})_6(\text{L}_1)_6](\text{NO}_3)_2$ (**2**)

To a solution of $\text{Co}(\text{NO}_3)_2 \cdot 6\text{H}_2\text{O}$ (0.25 g, 0.86 mmol) in MeOH (30 cm^3) was added 2-iminomethyl-6-methoxyphenol (0.142 g, 0.86 mmol). Solid NaOH (0.034 g, 0.86 mmol) was then added and the solution stirred at ambient temperature for 3 hours. The solution was then filtered to afford a dark red-brown mother liquor which was allowed to slowly evaporate to encourage crystallisation. Aliquots of the mother liquor were also diffused with diethyl ether (Et_2O) towards better quality crystals suitable for X-ray analysis. Dark brown/black hexagons of **2** were obtained both from slow evaporation and diethyl ether diffusion of the mother liquor with a combined yield of 30%. Elemental analysis calculated for $\text{C}_{56}\text{H}_{66}\text{N}_8\text{O}_{26}\text{Co}_7$ (%): C 40.04, H 3.96, N 6.67; Found: C 40.22, H 3.68, N 6.95. FT-IR (cm^{-1}): 3622(w), 3427(w), 2911(w), 2812(w), 1626(m), 1603(w), 1561(w), 1457

(m), 1438(m), 1407(w), 1334(m), 1304(m), 1241(m), 1221(s), 1168(w), 1091(w), 1073(m), 1032(m), 1012(m), 959(m), 858(w), 829(w), 784(w), 743(s), 683(w). UV/vis data [λ_{max} , nm (ϵ_{m} , $10^3 \text{ dm}^3 \text{ mol}^{-1} \text{ cm}^{-1}$) in MeOH: 352 (20.4), 262 (44.6), 233 (90.8); $[\text{CH}_3\text{CN}]$: 352 (20.3), 262 (48.8), 230 (107.3), 200 (107.7).

Preparation of 2-iminophenyl-6-methoxyphenol (L_2H) (**3**)

Modified from published methods:^{17b} To a solution of *o*-vanillin (2.0 g, 13.14 mmol) in EtOH (40 cm^3) was added distilled aniline (2.0 cm^3 , 21.94 mmol), yielding a bright orange solution. The solution was refluxed for 2 hours after which the solvent was removed *in vacuo*. This yielded a dark orange oil. To the oil was added a 1 : 1 Et_2O -acetone mix (total volume of 50 cm^3) and the solvent again removed *in vacuo*. The dark orange oil persisted and thus Et_2O (50 cm^3) only was added to the oil yielding a golden orange solution. The desired solid product (bright orange) soon began to crystallise out of solution. The mixture was placed in a fridge overnight (at a temperature of $\sim 2-3^\circ\text{C}$) to encourage further crystallisation of the desired product. The solid was isolated *via* filtration over a sintered glass frit and washed with the minimum volume of cold Et_2O . The product was received as bright orange crystalline blocks/plates in 83% yield. Elemental analysis calculated for $\text{C}_{14}\text{H}_{13}\text{N}_1\text{O}_2$ (%): C 73.98, H 5.77, N 6.17; found: C 73.64, H 5.36, N 5.77. FT-IR (cm^{-1}): 2955(w), 2909(w), 2837(w), 1612(s), 1586(m), 1462(s), 1409(w), 1361(w), 1329(w), 1250(s), 1194(s), 1090(w), 1075(m), 1023(w), 999(w), 966(s), 910(w), 886(w), 857(w), 832(w), 810(m), 781(s), 765(s), 735(s), 724(s), 689(s). ^1H NMR: (500 MHz, CDCl_3): δ 13.60 (s, 1H, OH), δ 8.62 (s, 1H, H-C=N), δ 7.66 (m, 8H, Ar), δ 2.95 (s, 3H, $\text{CH}_3\text{-O}$). UV/vis data [λ_{max} , nm (ϵ_{m} , $10^3 \text{ dm}^3 \text{ mol}^{-1} \text{ cm}^{-1}$)] in MeOH: 312 (16.8), 278 (13.2), 225 (25.5); $[\text{CH}_3\text{CN}]$: 309 (17.6), 277 (17.5), 226 (30.7), 207 (25.1).

$(\text{NO}_3)_2 \subset \text{Co}(\text{III})\text{Co}(\text{II})_6(\text{OH})_6(\text{L}_2)_6](\text{NO}_3) \cdot 3\text{MeCN}$ (**4**)

To a solution of $\text{Co}(\text{NO}_3)_2 \cdot 6\text{H}_2\text{O}$ (0.25 g, 0.86 mmol) in MeOH (30 cm^3) was added 2-iminophenyl-6-methoxyphenol (L_2H) (0.195 g, 0.86 mmol) initially affording a dark red-coloured, transparent solution, which gradually adopted a darker colour as stirring proceeded. Solid NaOH (0.034 g, 0.86 mmol) was then added resulting in the solution adopting a golden red-brown appearance. The solution was stirred for a further 5 h after which it was filtered, to yield a dark red-brown mother liquor. The product **4** was allowed to crystallise from the mother liquor *via* slow solvent evaporation. Complex **4** was received as dark red-brown crystalline blocks in 15% yield. Elemental analysis calculated for $\text{C}_{84}\text{H}_{78}\text{N}_9\text{O}_{27}\text{Co}_7$ (loss of all MeCN) (%): C 49.02, H 3.82, N 6.13; found: C 48.85, H 3.68, N 6.16. FT-IR (cm^{-1}): 3361(w), 1610(s), 1589(s), 1559(m), 1464(s), 1390(s), 1345(m), 1297(s), 1233(s), 1188(s), 1102(m), 1078(m), 1038(w), 1022(w), 972(m), 907(w), 848(w), 776(s), 733(s), 694(s). UV/vis data [λ_{max} , nm (ϵ_{m} , $10^3 \text{ dm}^3 \text{ mol}^{-1} \text{ cm}^{-1}$)] in MeOH: 364 (27.6), 276 (97.4), 226 (122.9), 204 (149.6); $[\text{CH}_3\text{CN}]$: 360 (32.2), 273 (97.4), 224 (164.5), 200 (226.4).

[Co(II)(L₂)₂] (5)

To a solution of CoSO₄·7H₂O (0.25 g, 0.89 mmol) in MeOH (25 cm³) was added L₂H (0.202 g, 0.89 mmol). The solution was stirred to afford complete dissolution of the solid material. Solid NaOH (0.036 g, 0.89 mmol) was then added which resulted in a dark red–brown solution. This solution was then stirred for a further 3 h under ambient conditions after which it was filtered to yield a dark red–brown solution. The solution was then placed in a fridge (at ~4 °C). Dark red–brown crystalline blocks of **5** were isolated from the mother liquor in moderate yield (20%) after 4 days. Elemental analysis calculated (%) for C₂₈H₂₄N₂O₄Co₁: C 65.73, H 4.73, N 5.47; found: C 65.71, H 4.64, N 5.68. FT-IR (cm⁻¹): 1602(s), 1578(s), 1539(m), 1487(m), 1463(m), 1431(s), 1386(m), 1356(w), 1323(m), 1228(s), 1186(s), 1106(m), 1076(m), 1028(w), 999(w), 980(m), 905(w), 866(w), 852(m), 786(m), 773(m), 762(m), 743(s), 691(s).

[Co(III)₂Na(II)₁(L₃)₆](BF₄) (6)

To an EtOH solution (25 cm³) of Co(BF₄)₂·6H₂O (0.25 g, 0.73 mmol) was added L₃H (0.179 g, 0.73 mmol). The solution was stirred for 5 min before NaOH (0.029 g, 0.73 mmol) was added to afford an opaque brown solution. The solution was further stirred for 5 h and then filtered affording a dark red–brown mother liquor. Following the lack of crystallisation of **6**, the solution was allowed to evaporate to dryness to afford a brown–black residue. This solid was then redissolved in MeCN (10 cm³) from which X-ray quality crystals of **6** were obtained (in 25% yield) upon Et₂O diffusion after 2 weeks. Elemental analysis calculated (%) for C₅₄H₅₄N₆O₁₂B₁F₄Br₆Co₂Na₁: C 38.47, H 3.23, N 4.98; found: C 38.26, H 3.44, N 5.03. FT-IR (cm⁻¹): 1628(s), 1590(w), 1546(w), 1463(m), 1452(m), 1435(s), 1354(w), 1342(w), 1307(s), 1238(s), 1217(m), 1189(w), 1098(m), 1080(m), 1052(m), 1027(m), 1018(m), 978(m), 960(w), 935(w), 874(m), 851(w), 834(m), 825(m), 787(m), 758(m), 689(s), 666(w).

Acknowledgements

The authors would like to thank the NUI Galway Millennium Fund (LFJ), the Irish Research Council (IRCSET) Embark Fellowship (SM) and the NUI Galway College of Science Fellowship (CMcD) for funding. EKB acknowledges the support of the EPSRC and the Leverhulme Trust.

References

- (a) D. J. Cram and J. M. Cram, *Container Molecules and their Guests*, Royal Society of Chemistry, UK, 1994; (b) D. R. Turner, A. Pastor, M. Alajarin and J. W. Steed, *Molecular Containers: Design Approaches and Applications*, in *Structure and Bonding*, Springer-Verlag, 2004, vol. 108, pp. 97–168; (c) Y. Liu, C. Hu, A. Comotti and M. D. Ward, *Science*, 2011, **333**, 436–440.
- (a) I. Stibor, *Topics in Current Chemistry: Anion Sensing*, Springer, 2005; (b) J. Perez and L. Riera, *Chem. Soc. Rev.*, 2008, **37**, 2658–2667 and references therein (c) J. Steed, *Chem. Soc. Rev.*, 2009, **38**, 506–519 and references therein.
- (a) L. M. Hancock and P. D. Beer, *Chem.–Eur. J.*, 2009, **15** (1), 42–44; (b) L. M. Hancock, L. C. Gilday, S. Carvalho, P. J. Costa, V. Felix, C. J. Serpell, N. L. Kilah and P. D. Beer, *Chem.–Eur. J.*, 2010, **16** (44), 13082–13094.
- M. Yoshizawa, J. K. Klosterman and M. Fujita, *Angew. Chem., Int. Ed.*, 2009, **48**, 3418–3438 and references therein.
- (a) W. P. Jencks, *Catalysis in Chemistry and Enzymology*, McGraw-Hill, New York, 1969; (b) R. Breslow, *Acc. Chem. Res.*, 1995, **28**, 146–153; (c) A. Kirby, *Angew. Chem., Int. Ed. Engl.*, 1996, **35**, 706–724.
- O. Danylyuk and K. Suwinska, *Chem. Commun. (Feature Article)*, 2009, 5799–5813.
- M. V. Rekharsky, T. Mori, C. Yang, Y. Ho Ko, N. Selvapalam, H. Kim, D. Sobransingh, A. E. Kaifer, S. Liu, L. Isaacs, W. Chen, S. Moghaddam, M. K. Gilson, K. Kim and Y. Inoue, *Proc. Natl. Acad. Sci. U. S. A.*, 2007, **104** (52), 20737–20742.
- (a) S. J. Dalgarno, P. K. Thallapally, L. J. Barbour and J. L. Atwood, *Chem. Soc. Rev.*, 2007, **36**, 236–245; (b) P. K. Thallapally, B. P. McGrail, S. J. Dalgarno, H. T. Schaef, J. Tian and J. L. Atwood, *Nat. Mater.*, 2008, **7**, 146–150.
- I. Imar, J. Hernando, D. Ruiz-Molina and D. MasPOCH, *Angew. Chem., Int. Ed.*, 2009, **48**, 2325–2329.
- For examples see: (a) T. Heinz, D. M. Rudkevich and J. Rebek Jr, *Nature*, 1998, **394**, 764–766; (b) F. Perret and A. W. Coleman, *Chem. Commun. (Feature Article)*, 2011, **47**, 7303–7319.
- (a) J. L. Atwood, E. K. Brechin, S. J. Dalgarno, R. Inglis, L. F. Jones, A. Mossine, M. J. Paterson, N. P. Power and S. J. Teat, *Chem. Commun.*, 2010, **46**, 3482–3486; (b) S. M. Taylor, G. Karotsis, R. D. McIntosh, S. Kennedy, S. J. Teat, C. M. Beavers, W. Wernsdorfer, S. Piligkos, S. J. Dalgarno and E. K. Brechin, *Chem.–Eur. J.*, 2011, **17**, 7521–7530; (c) S.-Y. Yu, H. Huang, H.-B. Liu, Z.-N. Chen, R. Zhang and M. Fujita, *Angew. Chem., Int. Ed.*, 2003, **42**, 686–690.
- (a) H. Amouri, C. Desmarests, A. Bettoschi, M. N. Rager, K. Boubekour, P. Rabu and M. Drillion, *Chem.–Eur. J.*, 2007, **13**, 5401–5407; (b) E. Pardo, K. Bernot, F. Lloret, M. Julve, R. Ruiz-Garcia, J. Pasan, C. Ruiz-Perez, D. Cangussu, V. Costa, R. Lescouezec and Y. Journaux, *Eur. J. Inorg. Chem.*, 2007, 4569–4573; (c) R. G. Harrison, J. L. Burrows and L. D. Hansen, *Chem.–Eur. J.*, 2005, **11**, 5881–5888.
- References (a) and (b) here formed part of a *Chem. Soc. Rev.* themed issue on *Hybrid Materials* which should also be considered here. (a) M. Clemente-Leon, E. Coronado, G. Marti-Gastaldo and F. M. Romero, *Chem. Soc. Rev.*, 2011, **40**, 473–497; (b) J. Yuan, Y. Xu and A. H. E. Muller, *Chem. Soc. Rev.*, 2011, **40**, 640–655.
- (a) S. T. Meally, C. McDonald, G. Karotsis, G. S. Papaefstathiou, E. K. Brechin, P. W. Dunne, P. McArdle, N. P. Power and L. F. Jones, *Dalton Trans.*, 2010, **39**, 4809–4816; (b) S. T. Meally, G. Karotsis, E. K. Brechin, G. S. Papaefstathiou, P. W. Dunne, P. McArdle and L. F. Jones, *CrystEngComm*, 2010, **12**, 59–63.
- (a) D. Altermatt and I. D. Brown, *Acta Crystallogr.*, 1985, **B41**, 244–247; (b) I. D. Brown, *Chem. Rev.*, 2009, **109**, 6858–6919.
- For examples see: (a) S.-H. Zhang, Y. Song, H. Liang and M.-H. Zeng, *CrystEngComm*, 2009, **11**, 865–872; (b) L.-Q. Wei, B.-W. Li, S. Hu and M.-H. Zeng, *CrystEngComm*, 2011, **13**, 510–516. Note: The {Co(II)₄-Co(III)₃} analogue to this work has previously been observed and should be noted here: A. Ferguson, A. Parkin, J. Sanchez-Benitez, K. Kamenev, W. Wernsdorfer and M. Murrie, *Chem. Commun.*, 2007, 3473–3475.
- (a) C. Albayrak, B. Koşar, S. Demir, M. Odabaşoğlu and O. Büyükgüngör, *J. Mol. Struct.*, 2010, **963**, 211–218; (b) G.-Y. Yeap, S.-T. Ha, N. Ishizawa, K. Suda, P.-L. Boey and W. A. K. Mahmood, *J. Mol. Struct.*, 2003, **658**, 87–100.
- Sh. Yue, J. Li Zh., H. Yu, Q. Wang, X. P. Gu and Sh. L. Zang, *Russ. J. Coord. Chem.*, 2010, **36** (7), 547–551.
- P. Viswanathamurthi, N. Dharmaraj and K. Natarajan, *Synth. React. Inorg. Met.-Org. Chem.*, 2000, **30**, 1273–1286.
- X. Li, F. Yu, H. Sun, L. Huang and H. Hou, *Eur. J. Inorg. Chem.*, 2006, **21**, 4362–4367.
- M. Moragues-Canovas, C. E. Talbot-Eeckelaers, L. Catala, F. Lloret, W. Wernsdorfer, E. K. Brechin and T. Mallah, *Inorg. Chem.*, 2006, **45**, 7038–7040.
- J. M. Clemente-Juan, E. Coronado, A. Forment-Aliaga, J. R. Galan-Mascaros, C. Saiz-Gimenez and J. C. Gomez-Garcia, *Inorg. Chem.*, 2004, **43**, 2689.
- (a) G. T. T. Cooper, G. N. Newton, P. Kogerler, D.-L. Long, L. Engelhardt, M. Luban and L. Cronin, *Angew. Chem., Int. Ed.*, 2007, **46**, 1340–1344; (b) X.-T. Wang, B.-W. Wang, Z.-M. Wang, W. Zhang and S. Gao, *Inorg. Chim. Acta*, 2008, **361**, 3895–3902.